Article

Polymer Nanofiber Mats for Electrochemical Sensing

Paloma Vilchis-León[*1], Josué Hérnandez-Varela[2], Jorge Chanona-Pérez[2], Raúl Borja Urby[3], Rodolfo Estrada-Guerrero[1]

[1] Laboratorio de Nanociencia y Nanotecnología, Departamento de Física y Matemáticas, Universidad Iberoamericana, Ciudad de México, México
[2] Laboratorio de Micro y Nano-Biotecnología, Departamento de Ingeniería Bioquímica, Escuela Nacional de Ciencias Biológicas, Instituto Politécnico Nacional, Ciudad de México, México.
[3] Center of Micro and Nanotechnology of IPN, in Mexico City
* Correspondence: paloma.vilchis01@correo.uia.mx.

Abstract

Polyvinyl alcohol (PVA) is highly compatible polymer with biological environments. Specifically, it has been used as a trap for different types of microorganisms in Bio-MEMS, and its properties can be modified to act as an electrode for electrochemical analysis. This study presents a nanocomposite developed with PVA, multiwall carbon nanotubes (CNTs) doped with nitrogen, which changes the electrical properties of the polymer and its viscosity to obtain nanofibers by electrospinning. The proposed nanocomposite was characterized using Fourier transform-infrared and Raman spectroscopy techniques, confirming the presence of the CNTs immersed in the polymer. High-resolution transmission electron microscopy was used to obtain the micrographs that showed the characteristic interplanar distances of the multiwall CNT in the polymeric matrix with values of 3.63 Å. Finally, the CNx mats were exposed to various aqueous solutions in a potentiostat to demonstrate the effectiveness of the nanofibers for electrochemical analysis. The CNx-induced changes in the electrical properties of the polymer were identified using cyclic voltammograms, while the electrochemical analysis revealed supercapacitor behavior.

Keywords: PVA, Nanofibers, CNx, Electrospinning, Electrochemical

1. Introduction

Electrospinning is an inexpensive method to obtain micro- and nanofibers [1,2]. A sufficiently high voltage is applied to a liquid to initiate electrospinning, which starts to accumulate charge, forming droplets until it reaches a conical form known as a Taylor cone. Fiber size is determined by the distance between the collector plate and the Taylor cone, the voltage, and the viscosity of the liquid [3,4].

Normally, liquid polymers are used for electrospinning. In general, polymers are not conductors; however, carbon nanotubes (CNTs) and particularly multiwall carbon nanotubes (MWCNTs) can increase the electrical properties of the polymer and decrease its viscosity [5]. Natural base polymers are multifaceted materials and their application in biomedical industries is growing rapidly, for example, in the development of point-of-care devices that can be used for sensing different kinds of pathogens. In particular, the biocompatibility of PVA makes it an ideal candidate for the synthesis of matrix traps for bioecological materials [6].

The electrospinning process has provided a low-cost alternative to fabricate biosensors, especially those focused on electrochemical sensing. The electrochemical biosensors have

been demonstrated to have an application in food technologies, biomedical areas, water filtration [7], and more recently in the recognition of biomolecules.

The recognition is possible thanks to the modification of electrodes with mats of nanofibers, in combination with screen-printed electrodes. This work presents an alternative using a commercial electrode cover with nanofibers made of a nanocomposite of polyvinyl alcohol, surfactant, and multiwall carbon nanotubes for further uses in biological sensing.

2. Materials and Methods

Materials

The main components of the proposed nanocomposite, namely PVA (98% hydrolyzed, average molecular weight of 72000 g mol^{-1}) and functionalized nitrogenate carbon nanotubes (CNx), were synthesized for the research group of nanoscience and nanotechnology at Iberoamericana University. Raw nitrogenate carbon nanotubes were used as reference material. Sodium dodecylbenzenesulfonate (NaDDBS), which was used as the surfactant, was purchased from Sigma Aldrich. Distilled water was used for all processes.

Electrospinning procedures

Solutions of PVA and NaDDBS were prepared separately. The latter was prepared with 5ml of dH_2O, 50mg of NaDDBS and 1 g of CNx, the solution was sonicated and stirred for three cycles lasting 30 min each. For the PVA solution, a 10% (v/v) concentration was used. Then, both solutions were mixed on a hot plate, while being stirred to avoid CNx aggregation and clusters of PVA to obtain the required viscosity for electrospinning and was added to achieve an 8.695% v/v in the finale solution.

Electrospinning was performed with a syringe pump (Kd Scientific) in a 5 mL syringe, with a velocity of 0.5 μL/min; the distance between the collector plate and the syringe tip was 15 cm. The process was performed at 10 kV using two power supplies connected in series. Nanofiber mats were obtained after 40 min of running the pump, checking that the viscosity remained constant and the tip residue-free.

Fourier transform-infrared (FT-IR) spectroscopy

To characterize the chemical groups in the polymer, surfactant, and CNx, FT-IR spectra were obtained using a Nicolet i10s FT-IR spectrometer (Thermo Scientific, USA). Spectra were obtained separately for CNx as a powder, one mat of nanofibers made with the nanocomposite, and another nanofiber mat made of PVA alone. All spectra were recorded in the range of 4000–650 cm^{-1}, and 20 scans were taken for four samples of each material. The spectra were recorded at a resolution of 4 cm^{-1} and normalized at 1030 cm^{-1}.

Raman spectroscopy

Raman spectroscopy was performed using a LabRam HR 800 Raman spectrometer (Horiba Jobin Yvon, Japan) coupled to an Olympus BX 41 microscope with a 100× objective. Raman spectra were recorded using a 600 lines/mm grating and a 653 nm emission laser. The spectral resolution was approximately 4 cm^{-1}. The measurements were conducted spanning the 100–3200 cm^{-1} wavenumber and using exposure times of 8–10 s, in the range of 19ºC of temperature.

Electron microscopy

For scanning electron microscopy (SEM), small samples of the mats were cut and examined using a Hitachi SU-3500 (Japan) instrument under high vacuum conditions. Images were acquired using the secondary electron detector. The samples were analyzed using slow frame rates of 3 and 15 Hz and a working distance of 6 mm. Furthermore, SEM images were used to evaluate the average fibers diameter (AFD) by measuring each fiber size with the length tool of ImageJ software version 1.47 (http://imagej.nih.gov; National

Institute of Health, Bethesda, MD, USA). The collected data were plotted as frequency histograms and adjusted to a gaussian distribution function in SigmaPlot software v 12.0 (Systat Software Inc., San Jose, CA, USA). The goodness of fit of the models was evaluated by their coefficient of determination (R^2). For high-reoslution transmission electron microscopy (HR-TEM), the mats were scraped, some of the nanofibers were wet with a droplet of isopropyl alcohol and deposited onto a cooper grid for transmission electron microscopy then let dry for 15 minutes. The TEM (JEOL, USA) was operated in bright-field mode at 80 kV to increase the contrast between CNx and the surrounding polymeric matrix [1, 8]. Micrographs were analyzed in GMS 3 software package (Gatan Microscopy, USA) using the methodology propose by Hernández-Varela [9], Images were processed by using Fast Fourier Transformation (FFT) for the crystalline regions (CR) of the sample. Then, an Inverse Fast Fourier Transformations (IFFT) was produced using the crystalline fringe of the reciprocal space from a particular mask, to produce a higher resolution representation of the interplanar distances. Finally, images were stored in TIFF format and used for discussion.

Electrochemical characterization

Electrochemical characterization of the fabricated PVA/CNT/NaDBBS nanofiber composite was performed using a potentiostat/galvanostat PGSTAT101 (Metrohm Autolab, Utrecht, Netherlands) connected to a PC with NOVA software used to control the potential, data acquisition, and treatment. The experiments were conducted using a conventional electrochemical cell with a three-electrode adaptation connector. For comparison, commercial electrodes (screen printed electrodes) and a mat of nanofibers made only with PVA were used in the analysis. The electrodes were characterized using a solution composed of 0.1 mol L^{-1} potassium ferricyanide ($K_3Fe(CN)_6$) and potassium ferrocyanide ($K_4Fe(CN)_6$) in 1 mol L^{-1} KCl, as well as, 1 mol L^{-1} KCl as control electrolyte. The electrochemical window was stablished between -0.2 and 0.6 V and a 10 scan rate. All reactants were analytical grade and had undergone no previous purification. The solutions were prepared in Milli-Q water (18.2 MΩ cm; Millipore Corporation, USA).

3. Results and discussion

Characterization of CNx

Figure 1 presents a Raman spectrum, acquired at 653 nm excitation, collected from raw nitrogenate carbon nanotubes (CNx) and functionalized nitrogenate carbon nanotubes (CNx-F) in powder form. The radial breathing modes (RBM) associated with large-diameter tubes are too weak to be observed in these spectra (100–200 cm^{-1})

[10]. The D-band shows a high-intensity peak at 1340 cm^{-1} corresponding to the induced disorder in the carbon nanotubes, and the G-band shows a tangential peak at 1586 cm^{-1}, which is related to the tangential E2g Raman active mode of graphite and caused by the tangential vibration of the two atoms in the graphene unit cell against each other [11]. In the second-order bands, a group of weak peaks can be observed between 2673 and 2955 cm^{-1}, which correspond to the G′ and D + G modes. For the D- and G-bands, functionalization caused a relative increase in the height of the bands. This behavior was expected, as chemical functionalization-induced increases in the D-band intensity have been reported in previous studies [12].

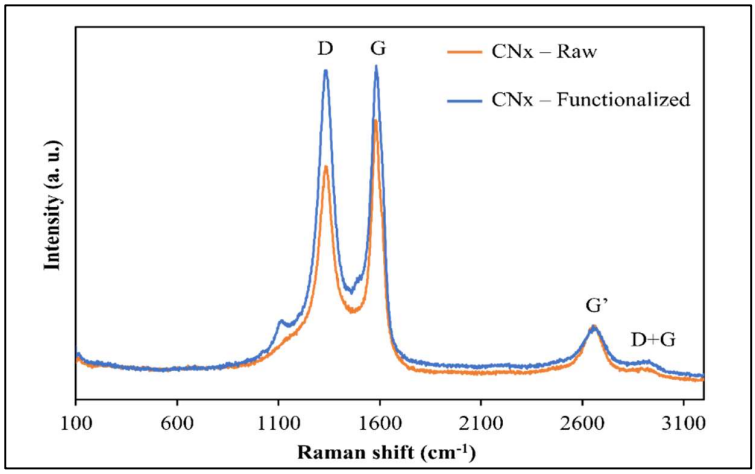

Figure 1. Raman spectra of raw and functionalized CNx.

Effect of surfactant on the dispersion of PVA/CNT/NaDBBS composite

CNTs have a high surface tension due to Van der Waal's interactions between them [2], provoking some aggregation problems due to the strength of these forces [10].However, some studies have shown that good CNT dispersion can be achieved by using a surfactant [13]. The surfactant reduces the surface tension of the CNTs, thus preventing aggregation. In addition, sonication can be used to achieve good dispersion in the solution, while several studies have reported that using a group of surfactants achieves good results [14, 15]. In all cases, NaDDBS was selected as an effective dispersant because it contains hydrophilic and hydrophobic parts that cause a double reaction when they are in solution [14, 16]. The hydrophobic part adsorbs on the CNT surface, while the hydrophilic part dissolves in the aqueous solution. Figure 2 shows a schematic representation of the interactions between CNTs, NaDDBS, and PVA in the final composite. The molecular chains of NaDDBS can be inserted between the disorganized CNT composite, creating a well-defined tridimensional grid when the CNTs are aligned and dispersed by the surfactant. Thus, by introducing a low-molecular-weight polymer, such as PVA, into the solution system, the PVA molecules can intercalate their structure in the CNT grid. As a consequence, a final composite comprising a PVA/CNT/NaDDBS solution was obtained, which was suitable for producing electrospun nanofibers.

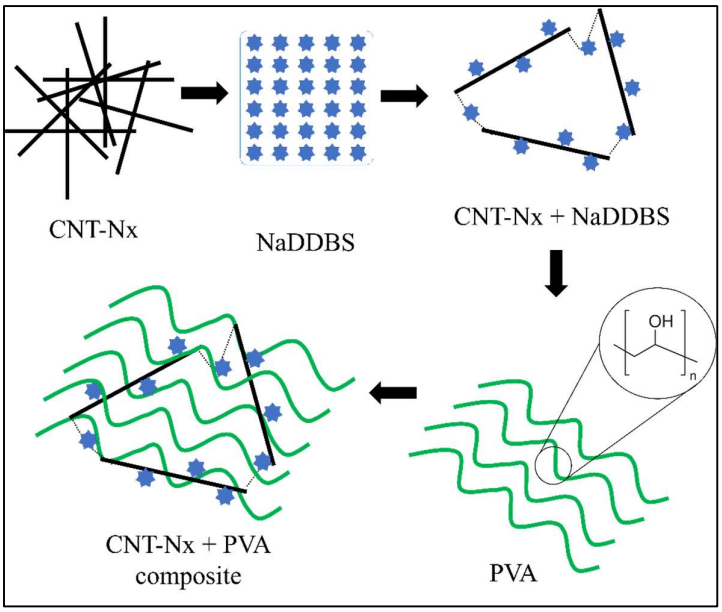

Figure 2. Schematic illustration of the interactions between CNT, NaDDBS, and PVA in the final composite.

Chemical and Physical Characterization of PVA/CNT/NADBBS Composite

Electrospun PVA and PVA/CNT/NaDBBS were observed using SEM. Figure 3 shows the SEM images of PVA and PVA/CNT/NaDBBS after 40 min of electrospinning, revealing their respective fiber diameter distributions. As shown in Figure 3A, in the pure PVA sample, the average fiber diameter was found to be in the range of 640 nm while in Figure 3B with 40 min of electrospinning, the average fiber diameter was 470 nm. From these micrographs, the role of the electrospinning time as a variable for achieving small nanofiber-based structures can be elucidated. The reduced diameter of the nanofibers in the composite is attributed to the increased stretching of the fibers during electrospinning, which was caused by the increased charge owing to the presence of conductive CNTs in the polymer solution. The diameters of electrospun fibers (Figure 3C, 3D) can range from several microns to tens of nanometers. Together, small fiber diameters and a large aspect ratio leads to an extremely high surface-to-volume (weight) ratio, which renders the electrospun nanofibers desirable for many applications, such as sensing devices [17].

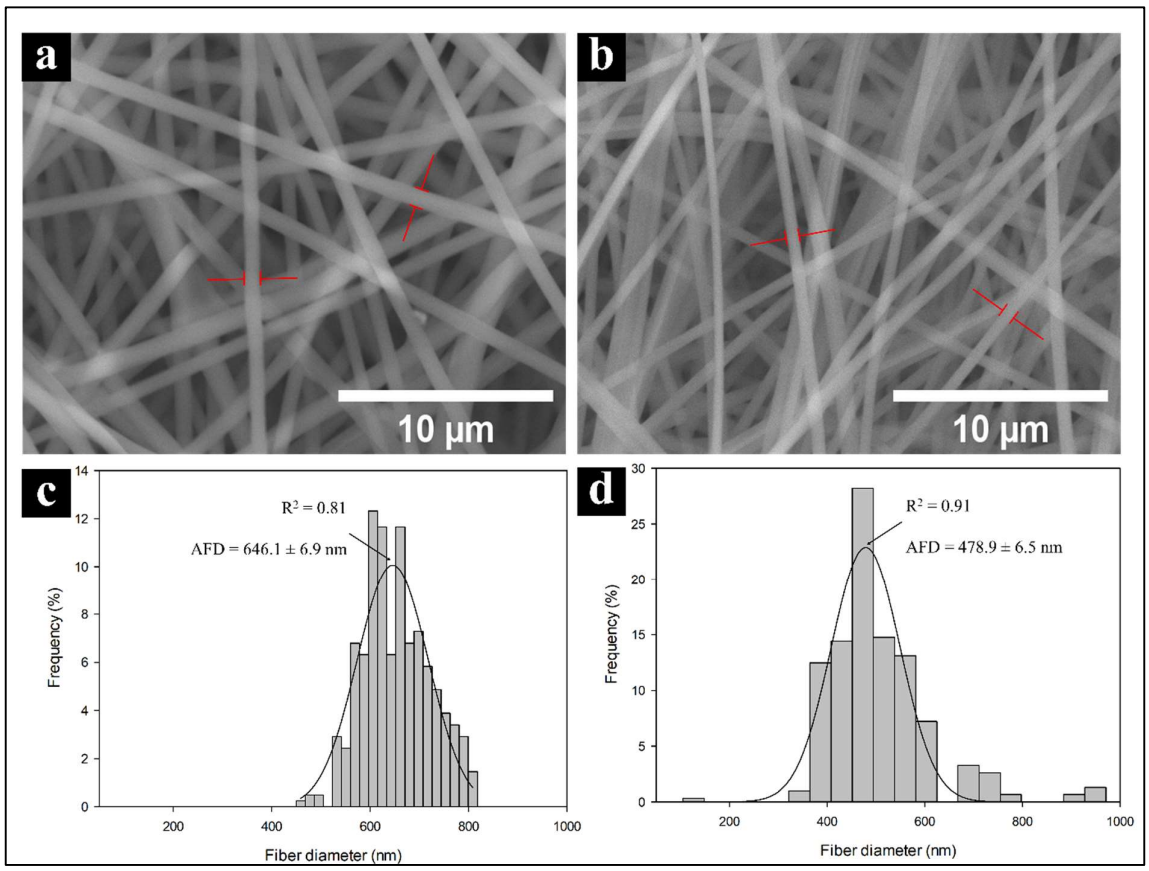

Figure 3. Scanning electron micrographs and histograms of fiber diameters for PVA nanofibers **(a, c)** and PVA + CNT_x nanofibers **(b, d).** AFD=average fiber diameters.

Next, FT-IR spectroscopy was used to assess the chemical groups in the polymers after electrospinning. Figure 4 shows the FT-IR spectra of PVA and PVA/CNT/NaDBBS after 40 min of electrospinning. In Figure 4, the major peaks in the FT-IR spectrum of PVA all relate to hydroxyl and acetate groups. More specifically, the broadband observed between 3400 and 3100 cm^{-1} is associated with the O–H stretching from inter- and intramolecular hydrogen bonds. The vibrational band observed between 2800 and 2980 cm^{-1} is the result of C–H stretching in alkyl groups, while the peaks between 1760 and 1510 cm^{-1} are due to the C=O and C–O stretching in the remaining acetate groups in PVA (owing to the saponification of PVA). Another characteristic peak of PVA below 1500 cm^{-1} corresponds to the C-C and C-O-C interactions in the polymeric matrix [17]. Other peaks at 823 cm^{-1} (–NH) and 642 cm^{-1} ($–NH_2$) result from the interactions between CNx and PVA in the matrix. Since normalization of the spectra at 1030 cm-1 is used to avoid false interpretation of the data, it seems that the dotted curve is a magnification of the solid curve, and these results suggest an interaction between CNx and the polymer matrix with the O–H group and -NH_2 groups involved in the composite [18].

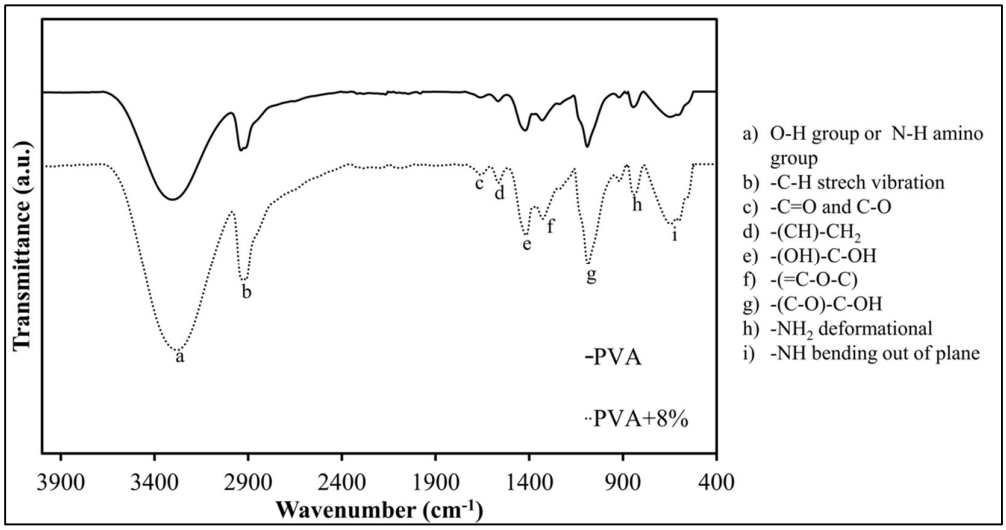

Figure 4. Fourier transform-infrared spectra highlighting the chemical groups in PVA (solid line) and PVA/CNT/NaDBBS (dotted line) after electrospinning.

In addition, Raman spectroscopy was used to evaluate the presence of CNTs and track the interactions of the composite after a time taken to obtain the mats. Figure 5 presents the Raman spectra of PVA and PVA/CNx/NaDBBS after 40 min of electrospinning. To understand the effect that adding the synthesized nitrogenate CNTs has on the internal structure of the composite, the Raman spectra of PVA with and without CNx are also shown in Figure 5. It can be seen that, except for the intrinsic ns(CH_2) stretch band at 2910 cm^{-1}, other characteristic band for pure PVA are observed at 1440 cm-1, 857 cm^{-1}, 912 cm^{-1} and 480 cm^{-1} [19]. However, when CNT loading levels were detected according to the characteristic peaks of CNT tangential modes, the well know D-band, G-band, G'-band suffers some shifted to values of 1364 cm^{-1}, 1602 cm^{-1}, and 2720 cm^{-1}, respectively [11, 19]. These displacements occur due to the stronger attachments of the CNx onto the polymeric matrix of the PVA and the influence of the surfactant in the CNx dispersion.

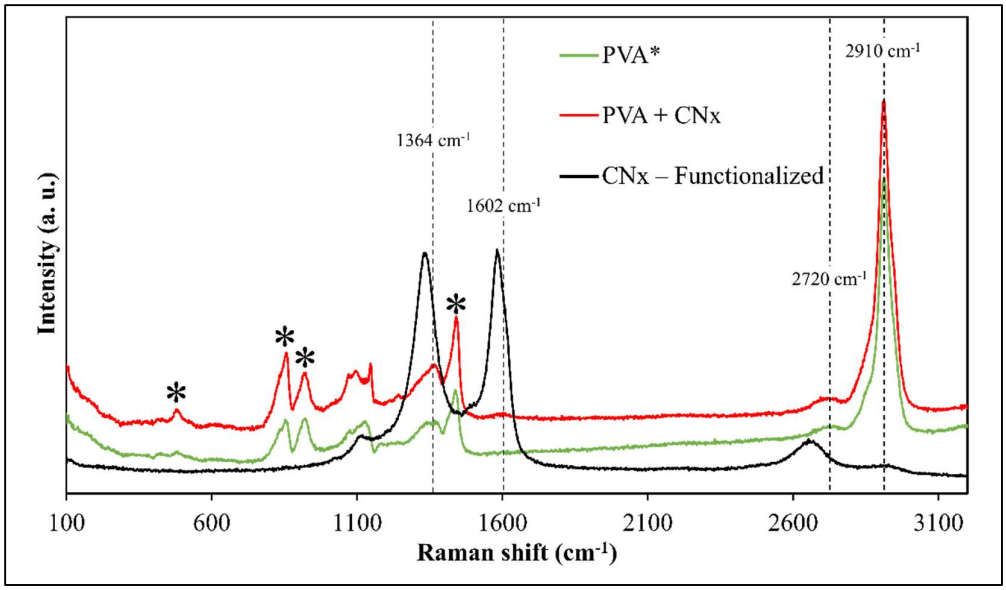

Figure 5. Raman spectra of PVA (green), PVA/CNx/NaDBBS (red), and CNx-functionalized (black). Black asterisk (*) represents the typical signal for PVA.

In other hand, some intrinsic factors, such as the polymer solution parameters (molecular weight, molecular weight distribution, electrical conductivity, surface tension, viscosity, and solvent type) and extrinsic factors, such as the operating parameters (electrical field, the distance from the nozzle tip and the collector, and the flow rate of the polymer) were evaluated in order to minimize the random errors in the production of the fibers but they were not included for discussion. Moreover, the ambient conditions were considered [4] to stablish the best way to obtain the mats.

Finally, a high-resolution analysis using TEM images was made to evaluate the interaction between polymer and CNx. Figure 6 shows an image of PVA/CNT/NaDBBS electrospun nanofibers and their high-resolution image analysis. Figure 6A shows the regular configuration of each nanofiber in polymer mats created with electrospinning. The nanofibers have sizes around 200 nm as it was show in SEM images; in contrast, Figure 6B shows the amplification of the inset selected in Figure 6A. As it was expected, some irregularities or amorphous regions (AR) are showed for PVA/NaDBBS material. However, crystalline regions are observed (CR) in Figure 6B attributed to bunches of nanotubes present in the intermolecular chain of PVA, provoking a regular surface morphology that is not observed in PVA. Using the selected region in Figure 6B (dashed square), an edge-on crystalline lamella was evaluated by applying a FFT. The crystalline region in the reciprocal space (inset, Figure 6B) was used to produce a mask and later on, produced a IFFT to measure the interplanar distance in the sample (Figure 6C). For this case of study, the interplanar distances on CNx were measured with the software and values of 3.63±0.23 Å were obtained. Similar results were found for interplanar distances of multi walled carbon nanotubes using HR-TEM. Singh et al. [20] reported values between 3.8-3.2 Å when CNT diameter sizes change from 5 to 100 nm.

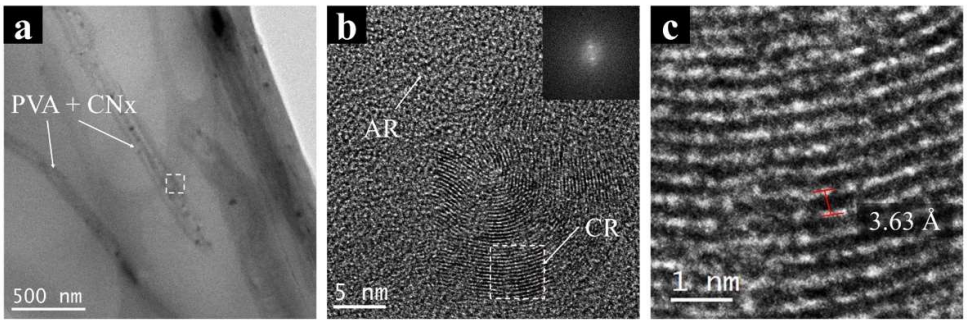

Figure 6. Transmission electron micrographs of (A) PVA + CNx nanofibers and (B) the magnification image of the nanocomposite showing their crystallographic structure. (C) Reconstruction of the FFT to a IFFT showing the interplanar distances in CNx. AR: amorphous regions; CR: crystalline regions.

Electrochemical Characterization

The current-potential characteristics experiments of three different samples were obtained using a commercial screen-printed electrode (solid line), with PVA (dotted line) and the nanocomposite (dashed line) showed in Figure 7. Cyclic voltammetry (CV) at XX mV/s in two solution used to characterize the electrodes was composed of 0.1 mol L^{-1} potassium ferricyanide ($K_3Fe(CN)_6$), 1 mol L^{-1} potassium ferrocyanide ($K_4Fe(CN)_6$), and 3 mol L^{-1} KCl. First, a commercial electrode (solid line) was used as a control response in the KCl solution at room temperature (Figure 7A), then another electrode was used and put on one section a small piece of PVA mat (dotted line), finally another electrode cover with the nanocomposite mat (dashed line), in the same KCl solution. The same experiment was conducted for the electrolyte solution $Fe(CN)_6^{-3}$ / $Fe(CN)_6^{-4}$ (Figure 7B).

Figure 7 shows the electrochemical responses for raw control electrodes, control electrodes with mat of PVA and PVA with CNx, int different aqueous solution. For a common electrolyte solution of KCl 1M (Figure 7A), the control electrode has almost cero respond (solid line), and the electrode just with PVA (dotted line), increase the conductivity of the

systems by introducing a small quantity of the surfactant that changes the electrical properties of the polymer. Nevertheless, it is important to control the addition of surfactant because high amount of surfactant could reduce the viscosity of the solution almost like water and could form micelles or aggregates. Finally, when CNx are added to the PVA mat, two characteristic peaks appear around +0.17V and -0.02V (dashed line) because the redox process involved in the system. It is important to explain that both peaks are missed in the electrode with just PVA and raw electrode, but the intensity of the peaks are not significant to evaluate the redox process in the systems. For that, a complex electrolyte solution based on potassium ferricyanide was used as shown Figure 7B. When the control electrode is evaluated (solid line), a classical response is presents in the electrochemical analysis, while the electrode with only PVA and the electrode with the PVA+CNx nanocomposite shows a reversible redox process. Particularly, the electrode with just PVA shows positive redox process at 0.18 and 0.05 V but the nanocomposite with PVA+CNx presents two peaks at +0.27V and -0.10V, which is a desirable value for an electrode conduct to sensing biological analytes.

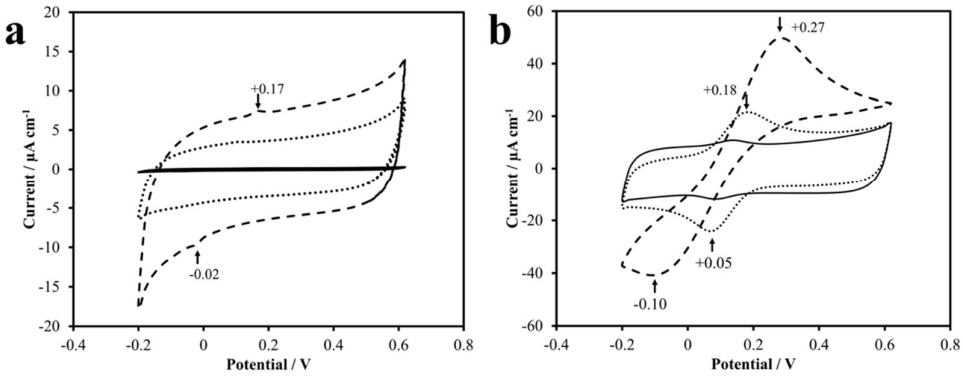

Figure 7. Electrochemical kinetics of PVA nanofibers on a screen-printed electrode. Cyclic voltammograms of the screen-printed electrode (solid line), pure PVA (dotted line), and PVA + CNx (dashed line), showing their electrochemical response to an aqueous solution of 1 M KCl (A) and $Fe(CN)_6^{-3}$ /$Fe(CN)_6^{-4}$ (B).

5. Conclusions

This study demonstrates that the use of CNx improves the electrical properties of the polymer, while the surfactant helps to obtain a solution with an appropriate viscosity for fabricating nanofiber mats.

These nanocomposite mats can be used as electrodes for electrochemical sensing. In addition, the nanofiber composite mats exhibit potential as supercapacitors. Therefore, these nanomaterials could be used as selective biosensors in Bio-MEMS for diagnostic purposes.

Author Contributions: All the authors listed made a substantial, direct contribution to the work and approved the final manuscript for publication.

Data Availability Statement: The raw data supporting the conclusions of this article will be made available by the author without undue reservation

Acknowledgments: To Dr. Felipe Cervantes and Rodrigo Cuevas, at the Nanotechnology and Nanosciencenanoscience Lab at Iberoamericana University. To CONACyT

Conflicts of Interest: The authors declare no conflict of interest.

References

1. Holmberg, S., Ghazinejad, M., Cho, E., George, D., Pollack B., Perebikovsky, A., Ragan, R., and Madou, M. (2018). Stress-Activated Pyrolytic Carbon Nanofibers for Electrochemical Platforms. *Electrochim. Acta* 290, 639–648.
2. Wongon, J., Thumsorn, S., and Srisawat, N. (2016). Poly(vinyl alcohol)/Multiwalled Carbon Nanotubes Composite Nanofiber. *Energy Procedia* 89: 313–317.
3. Naebe, M., Lin, T., Staiger, M. P., Dai, L., and Wang, X. (2008). Electrospun single-walled carbon nanotube/polyvinyl alcohol composite nanofibers: Structure-property relationships. *Nanotechnology* 19. doi:10.1088/0957-4484/19/30/305702.
4. Naebe, M., Lin, T., and Wang, X. (2010). Carbon Nanotubes Reinforced Electrospun Polymer Nanofibres. *Nanofibers*. doi:10.5772/8160.
5. Almecija, D., Blond, D., Sader, J. E., Coleman, J. N., and Boland, J. J. (2009). Mechanical properties of individual electrospun polymer-nanotube composite nanofibers. Carbon N. Y. 47, 2253–2258. doi:10.1016/j.carbon.2009.04.022.
6. Adewunmi, A. A., Ismail, S., and Sultan, A. S. (2016). Carbon Nanotubes (CNTs) Nanocomposite Hydrogels Developed for Various Applications: A Critical Review. *J. Inorg. Organomet. Polym. Mater.* 26 (4), 717–737.
7. Moradi, Mona, Maryam Azizi-Lalabadi, Parisa Motamedi, and Ehsan Sadeghi. 2021. "Electrochemical Determination of T2 Toxin by Graphite/Polyacrylonitrile Nanofiber Electrode." *Food Science & Nutrition* 9 (2): 1171–79.
8. Zhou, C., Liu, Z., Du, X., Mitchell, D. R. G., Mai, Y.-W., Yan, Y., and Ringer, S. (2012). Hollow Nitrogen-Containing Core/Shell Fibrous Carbon Nanomaterials as Support to Platinum Nanocatalysts and Their TEM Tomography Study. *Nanoscale Res. Lett.* 7 (1): 165.
9. Hernández-Varela, J. D., Chanona-Pérez, J. J., Calderón Benavides, H. A., Cervantes Sodi, F., and Vicente-Flores, M. (2021). Effect of ball milling on cellulose nanoparticles structure obtained from garlic and agave waste. Carbohydr. Polym. 255, 1–12. doi:10.1016/j.carbpol.2020.117347.
10. Guadarrama-Fernández, L., Chanona-Pérez, J., Manzo-Robledo, A., Calderón-Domínguez, G., Martínez-Rivas, A., Ortiz-López, J., et al. (2014). Characterization of functionalized multiwalled carbon nanotubes for use in an enzymatic sensor. Microsc. Microanal. 20, 1479–1485. doi:10.1017/S143192761401304X.
11. Murphy, H., Papakonstantinou, P., and Okpalugo, T. I. T. (2006). Raman Study of Multiwalled Carbon Nanotubes Functionalized with Oxygen Groups. *J. Vac. Sci. Technol. B.* 24 (2), 715.
12. Rebelo, S. L. H., Guedes, A., Szefczyk, M. E., Pereira, A. M., Araújo, J. P., and Freire, C. (2016). Progress in the Raman Spectra Analysis of Covalently Functionalized Multiwalled Carbon Nanotubes: Unraveling Disorder in Graphitic Materials. *Phys. Chem. Chem. Phys.* 18 (18), 12784–12796.
13. Crespo, G. A., Macho, S., Bobacka, J., and Rius, F. X. (2009). Transduction Mechanism of Carbon Nanotubes in Solid-Contact Ion-Selective Electrodes. *Anal. Chem.* 81 (2), 676–681.
14. Islam, M. F., Rojas, E., Bergey, D. M., Johnson, A. T., and Yodh, A. G. (2003). High weight fraction surfactant solubilization of single-wall carbon nanotubes in water. Nano Lett. 3, 269–273. doi:10.1021/nl025924u.
15. Kwon, O. S., Kim, H., Ko, H., Lee, J., Lee, B., Jung, C. H., et al. (2013). Fabrication and characterization of inkjet-printed carbon nanotube electrode patterns on paper. Carbon N. Y. 58, 116–127. doi:10.1016/j.carbon.2013.02.039.
16. Nasouri, K., Salimbeygi, G., Mazaheri, F., Malek, R., and Shoushtari, A. M. (2013). Fabrication of polyvinyl alcohol/multi-walled carbon nanotubes composite electrospun nanofibres and their application as microwave absorbing material. *Micro & Nano Lett.* 8, 455–459. doi:10.1049/mnl.2013.0381.
17. Alhosseini, S. N., Moztarzadeh, F., Mozafari, M., Asgari, S., Dodel, M., Samadikuchaksaraei, A., Kargozar, S., and Jalali, N. (2012). Synthesis and Characterization of Electrospun Polyvinyl Alcohol Nanofibrous Scaffolds Modified by Blending with Chitosan for Neural Tissue Engineering. *Int. J. Nanomed.* 7, 25–34.
18. Zamri, M. F. A., Zein, S. H. S., Abdullah, A. Z., and Basir, N. I. (2011). Improved electrical conductivity of polyvinyl alcohol / multiwalled carbon nanotube nanofibre composite films with MnO2 as filler synthesised using the electrospinning process. *Int. J. Eng. Technol.* 11, 20–26
19. Chen, W., Tao, X., Xue, P., and Cheng, X. (2005). Enhanced Mechanical Properties and Morphological Characterizations of Poly(Vinyl Alcohol)–Carbon Nanotube Composite Films. *Appl. Surf. Sci.* 252 (5), 1404–1409.
20. Singh, D. K., Iyer, P. K., and Giri, P. K. (2010). Diameter dependence of interwall separation and strain in multiwalled carbon nanotubes probed by X-ray diffraction and Raman scattering studies. *Diam. Relat. Mater.* 19, 1281–1288. doi:10.1016/j.diamond.2010.06.003.
21.